
Article:
Dube, C.L., Stennett, M.C. orcid.org/0000-0002-8363-9103, Ananthanarayanan, A. et al. (3 more authors) (2020) Radiation stability study on cerium loaded iron phosphate glasses by ion irradiation method. Journal of Radioanalytical and Nuclear Chemistry, 323 (3). pp. 1381-1386. ISSN 0236-5731

https://doi.org/10.1007/s10967-020-07012-z

Radiation stability study on cerium loaded iron phosphate glasses by ion irradiation method

Charu L. Dube[1*], M.C. Stennett[2], A. Ananthanarayanan[3], C. David[4], J. G. Shah[3], N.C. Hyatt[2]

[1]*School of Nano Sciences, Central University of Gujarat, Gandhinagar, India.*

[2] *Department of Materials Science and Engineering, University of Sheffield, Sheffield, UK.*

[3]*Nuclear Recycle Group, Bhabha Atomic Research Centre, Mumbai, India.*

[4]*Materials Science group, Indira Gandhi Centre for Atomic Research, Kalpakkam, India.*

Abstract

To study radiation stability of iron phosphate glasses, cerium is used as surrogate of actinides. Cerium doped iron phosphate glasses have been synthesised. Heavy gold ion irradiations have been performed on pure and cerium doped iron phosphate glasses to mimic ballistic damage due to cascade of recoil atoms. Pure and cerium doped glasses are irradiated with gold ions of energy 750keV at fluence of $2*10^{15}$ ions/cm^2. In this paper, ion irradiation effects on glass network modification and change in speciation of network former have been discussed. Significant changes in glass network structure and speciation of network former is observed.

Keywords

Radiation stability, iron phosphate glass, heavy ion irradiation, infrared spectroscopy, X-ray absorption spectroscopic measurements.

Introduction:

The global energy demand is going to increase manifold in coming years and fossil fuel stocks are limited in nature. To meet future energy requirements, we need to exploit all available alternative resources. Nuclear power is being seen as one of the promising source of

power. Nuclear power can be harnessed from both nuclear fusion and fission reactions without carbon dioxide emissions. Nuclear power reactors have capability to provide carbon free energy future. However, significant amount of nuclear waste gets generated from nuclear power reactors, which needs to be immobilised before permanent disposal. On the basis of radioactivity, nuclear wastes are classified mainly as (i) low level, (ii) intermediate level, and (iii) high level waste. High level waste (HLW) is only 3% in volume but it contributes more than 98% activity to the nuclear waste. HLW contains minor actinides and plutonium residues. Due to very high activity (10^7-10^{14} Bq/m^3), HLW needs to be vitrified in suitable matrix prior to permanent disposal [1].The vitrified nuclear waste form should be radiation and corrosion resistant. Radiation damage due to incorporated actinides can lead to crack formation in vitrified nuclear waste. The vitrified nuclear waste form should remain durable for million years in geological repositories. Cement lining will be present in all geological repositories. There is high probability for the cementitious water to reach the vitrified nuclear waste through radiation induced cracks in vitrified nuclear waste. Interaction of cementious water with vitrified nuclear waste can accelerate glass dissolution [2]. Dissolution of vitrified nuclear waste is point of concern as it poses threat for leakage of radionuclide to the environment. Therefore, it is imperative to study radiation stability of vitrified nuclear waste form.

Iron Phosphate glasses and Interaction with Ions

Nuclear waste contains multiple elements along with actinides. Glasses having ability to contain multiple elements are considered for disposal of the nuclear waste [3]. Phosphate glasses having low melting temperatures are potential candidate for nuclear waste immobilisation [4]. Under phosphate glasses, iron phosphate glasses (IPG) are being considered as potential matrix for vitrification of HLW containing minor actinides and plutonium residues [5]. Chemically durable iron phosphate glasses have been studied and it is found that chemical durability of 60 mole% P_2O_5-40 mole% Fe_2O_3 (IPG6040) is best among various compositions of the iron phosphate glasses [6].

Ion irradiation, as an alternative method, is being used to study radiation stability of nuclear waste forms [5, 7]. The advantages of ion irradiation method are the high damage rate and the process does not activate the matrix [7]. High damage rates helps in inducing life time

damage in vitrification matrix without sample activation. Irradiated samples are readily available for characterisation. The incorporated actinides undergo alpha decay and results in the formation of alpha-particles of energy in the range of 4.5 - 5.5 MeV; recoil nuclei of energy in the range of 70-100 keV; along with some gamma rays. The high energy alpha particles predominately deposit their energy by electronic losses. Energy deposition leads to ionization, and localized electronic excitation results into atomic motion. Consequently interaction of alpha particle with vitrifying matrix leads to the permanent displacement of atoms form their respective sites. The displacement damage is measured in units of displacements per atom (dpa). Simultaneously, the cascade of recoil nuclei having atomic weight of 235 - 244 deposit their energy through ballistic elastic collisions with the nuclei of atoms in the vitrifying matrix. The incident ion dislodges atoms in vitrifying matrix. This is known as primary knock off followed by secondary, tertiary and so on knock off depending upon ion energy and mass. The dislodging of atoms from their sites leads to depolymerisation of glass network. Hence modification of glass network is anticipated, which lead to changes in mechanical properties (communicated elsewhere else). Therefore, alpha particles as well as cascade of recoil nuclei potentially affects the structural integrity of vitrifying/immobilising matrix. The objective of present work is to study ion beam irradiation effects on glass structure and change in speciation of glass network former.

Due to similarity between cerium and plutonium in terms of electronic configuration redox properties, and ionic radii [8], cerium is used as surrogate of actinides (plutonium) to simulate waste loaded glass. Wang et al. have carried out detail study on cerium doped iron borophosphate glasses [8]. They have reported formation of CeO_2 doped iron borophosphate glass for CeO_2 upto 9 mole%. However, X-ray diffraction pattern of glass samples having CeO_2 upto 9 mole%, has shown partial crystallisation and XRD peaks confirm presence of $CePO_4$ crystals. Depolymerisation is also observed with doping of CeO_2.

Experimental Details

Iron phosphate glass of composition 60 mole% P_2O_5 and 40 mole% Fe_2O_3 (pure glass) and cerium doped pure glass was synthesised using $NH_4H_2PO_4$, Fe_2O_3 and CeO_2 as starting precursors. The starting precursors were taken in desired ratio. The precursors were mixed and transferred in recrystallized alumina crucibles. The crucible containing precursors was kept in furnace at 1150 ^{0}C for 4 hour for uniform heating. Cerium doped samples were

prepared having different mole% of CeO_2 (0 mole%, 3 mole%, 6 mole% and 9 mole %). The molten glass was cast into a steel mold and later on kept at 500 ^{0}C for 1 hour for annealing to relieve residual internal stresses. The bubble free glass sample was cut into discs by using glass cutting machine. The glass samples were polished upto 1 micron finish by using lapping and polishing machine. To mimic the damages caused by collision cascades of recoil nuclei (having atomic weight of 235-244 due to alpha decay of incorporated minor actinides), heavy gold ions of atomic weight 197 is chosen. Gold ions are having mass closer to that of recoil nuclei. The displacement damage due to nuclear stopping of gold ions in glass matrix at 750 keV ion energy obtained from SRIM/TRIM software is given in figure 1 [9]. Fluence of $2*10^{15}$ ions/cm^2 is chosen to get representative damage of nearly 6 dpa at depth of 150 nm as shown in figure 1. Pure and cerium doped glasses were irradiated with gold ions of energy 750keV at fluence of $2*10^{15}$ ions/cm^2 at IGCAR Kalpakkam.

The energy deposition by gold ions at energy of 750keV is mainly through nuclear losses. Gold ions of energy 750 keV, having mainly nuclear loss, will lead to displacement damage by knocking off the glass matrix atoms. The displacement energy for estimation of displacement damage using SRIM/TRIM software is taken as 50eV for Fe, P and O atoms and the glass density is taken as 2.8 g/cm^3 for $Fe_{0.8}P_{1.2}O_{4.2}$ composition.

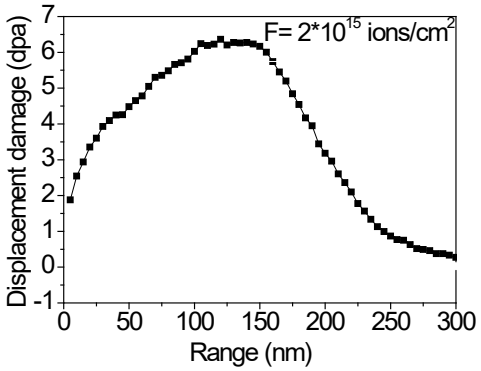

Fig. 1: The distribution of displacement damage inside glass sample

Before irradiation samples were characterized for their structural parameters by employing X-ray diffraction method and Raman spectroscopy. The electron microscopic images are taken on TM3030 SEM machine. The X-ray diffraction (XRD) patterns have been collected in θ-2θ geometry on D2 phaser machine, operating at voltage of 30kV and current of 10mA. Raman spectra in the range of 800 to1400 cm$^-$1 were collected by using inVia Raman microscope using excitation laser light of wavelength 514.5 nm. Measurements were carried out lower

power nearly 10mW to avoid damage to sample. The obtained Raman spectra were deconvoluted to see cerium induced modifications in the basic unit of IPG samples using WiRE software.

The pure and cerium doped IPG samples were characterised for their structural modifications before and after irradiation by using FTIR spectroscopy in specular reflectance mode. Specular reflectance spectroscopy is kind of mirror-like reflection from the sample surface, in which incident infrared radiation focused onto the sample surface gets reflected by the sample surface and give rise to specular reflection [10]. FTIR spectra of pure and irradiated glass samples were measured in the range 850 to1500 cm^{-1} using spectrophotometer (Perkin Elmer). The Kramer's–Koenig transformation is applied on obtained spectra to get normal absorption spectrum.

To investigate the irradiation induced changes in speciation of network former soft X-ray absorption spectroscopic (SXAS) measurements were carried out on beamline 1, Indus 2 at RRCAT, Indore in total electron yield (TEY) mode. Measurements have been carried out in soft X-ray regime, therefore the measured current is mainly due to emission Auger electrons from near surface region. The X-ray beam size at sample position is ~500µm X 500µm. Soft X-rays in regime of 700-740eV is used as binding energy of the 2p core level electron for iron is ~ 710eV. The observed spectra are calibrated to absorption maximum for Fe_2O_3 sample. In TEY mode SXAS measurements, current from the sample surface is measured with respect to the ground.

Results and discussion

X-ray measurements

The X-ray diffraction patterns for synthesised pure and CeO_2 doped iron phosphate samples are shown in figure 2. The amorphous hump is seen for 0 mole%, 3 mole%, 6 mole% and 9 mole%. CeO_2 doped IPG samples. However, significant crystallisation is seen for IPG sample having 9 mole% of CeO_2. Probably, limited solubility of CeO_2 in IPG glass matrix is responsible for observed crystallisation in samples having higher content of CeO_2. It is found that the crystals are mainly of $FePO_4$ and $CePO_4$. Wang *et al.* have also seen similar

crystallisation for iron borophosphate glass samples having higher doping concentrations of CeO_2 [7].

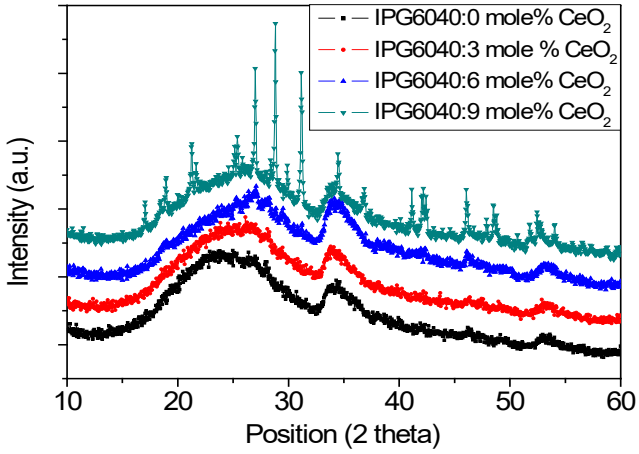

Fig. 2 X-ray diffractograms for pure and cerium doped IPG samples

Raman spectroscopic measurements

In order to see the effect of CeO_2 doping on glass network, Raman spectra were collected for 0 mole% and 3 mole% CeO_2 doped IPG glass samples. The Raman spectra recorded in the range of 800–1400 cm^{-1}.

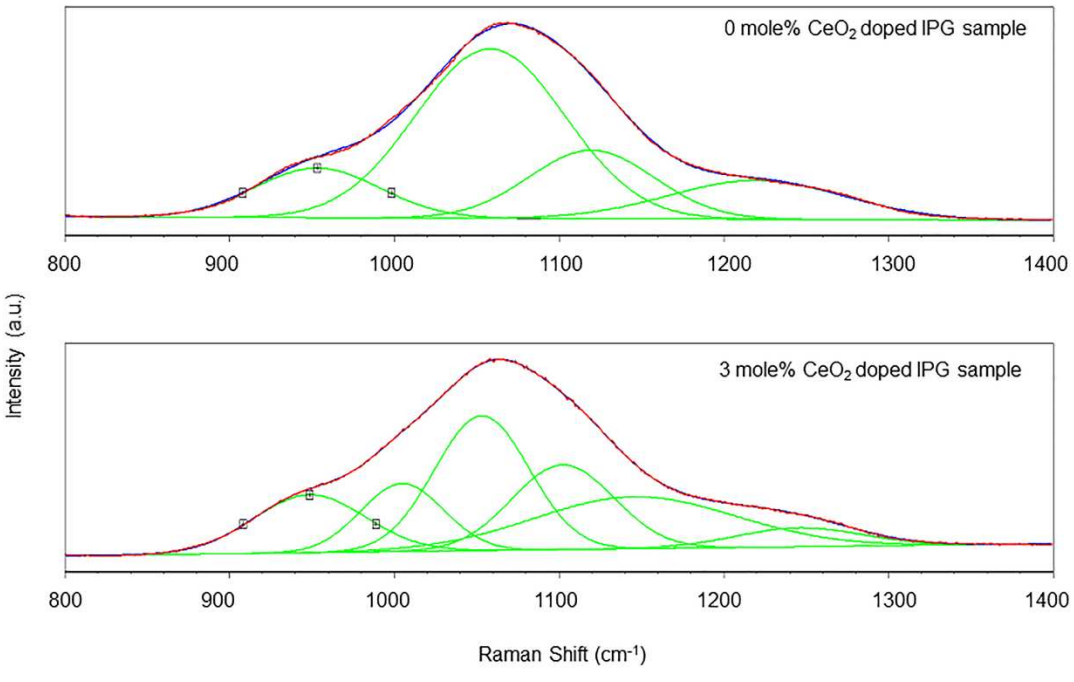

Fig. 3 Deconvoluted Raman spectra for pure and cerium doped IPG samples

The obtained spectra were fitted with Gaussian type function in WiRE software. The deconvoluted spectra for pure and CeO_2 doped iron phosphate glass samples are shown in figure 3.

As we can see in figure 3, for 0 mole% and 3 mole% CeO_2 doped glass samples, 4 and 7 peaks have been obtained, respectively. The Raman band assignments for cerium doped IPG samples are given in table 1. For 3 mole% CeO_2 doped glass samples, three new peaks appear at ~1005 cm^{-1} , ~1046 cm^{-1} and ~1255 cm^{-1}. The origin of theses peaks are given in table1. The detailed Raman study for IPG sample without doping can be found in our previous publication [5]. It is found that IPG6040 glass of composition $Fe_{0.8}P_{1.2}O_{4.2}$, contains mainly Q^1 species. To some extent, it also contains some Q^0 and Q^2 species. Lai *et al.* have performed detail spectroscopic study on CeO_2 doped iron phosphate glass samples. The obtained Raman spectrum for 3 mole% CeO_2 doped iron phosphate glass sample is in coherence to reported Raman spectrum for CeO_2 doped glass samples by Lai *et al.* [11].

Table 1 Active Raman absorption bands.

Wave number (cm^{-1})	Band assignment
946-952	Isolated $(PO_4)^{3-}$ stretch (Q^0) [5]
1002-1011	PO^- stretch (Q^0) [11]
1037-1064	$(PO_3)_{sym}$ stretch (Q^1) [11]
1105-1121	(PO_2)sym stretch (Q^2) [11]
1150-1176	Strained (PO_2)sym [11]

1213-1224	(PO_2)sym stretch (Q^2) [11]
1279-1296	(P=O)sym stretch [11]

Electron microscopic measurements

The electron microscopic images for 0 mole% and 3 mole% CeO_2 doped glass samples are shown in figure 4, taken at column voltage of 15kV. Images of secondary electron and back scattered electron for 3 mole% CeO_2 doped glass samples are shown in figure 4b and 4c. The microscopic images (figure 4) confirm formation of bubble free glasses. Phosphate crystals can be seen for 3 mole% CeO_2 doped IPG sample. However, crystallisation is not seen in X-ray diffraction pattern for 3 mole% CeO_2 doped IPG sample due to lower doping concentration and instrument detection limit.

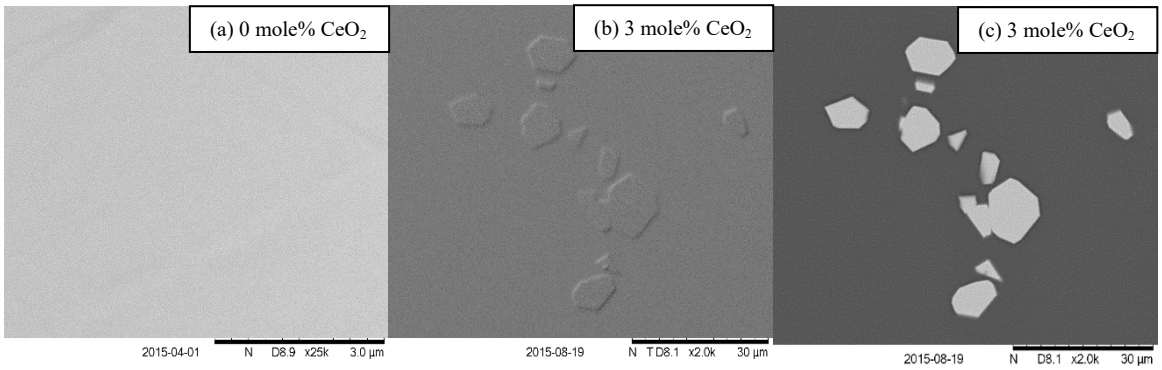

Fig. 4 Scanning electron images for (a) 0 mole% (b,c) for 3 mole% CeO_2 doped iron phosphate glass samples

As crystallisation is seen even in 3 mole% CeO_2 doped iron phosphate glass samples, therefore radiation stability study has been formed only on pure **(**0 mole%) and 3 mole% CeO_2 doped IPG samples.

It is evident from figure 1 that ion beam induced radiation damages are lying close to the sample surface, therefore characterisation of ion irradiation induced changes in glass network and specification of network former is challenging task. We need surface sensitive techniques for characterisation. The effect of irradiation on glass structure and speciation of network former is discussed in sections given below.

Infrared spectroscopic measurements

Specular reflectance spectroscopy is employed to characterise damages lying close to sample surface. Infrared spectroscopic spectra for the pure and 3 mole% CeO_2 doped IPG samples before and after irradiation are shown in figure 5. The detailed IR study for IPG6040 samples before and after irradiation can be found in our earlier publication [5]. In figure 5, grid lines are provided with respect to 0 mole% CeO_2 doped IPG samples for major absorbance peaks to see the doping and irradiation induced changes in glass network clearly.

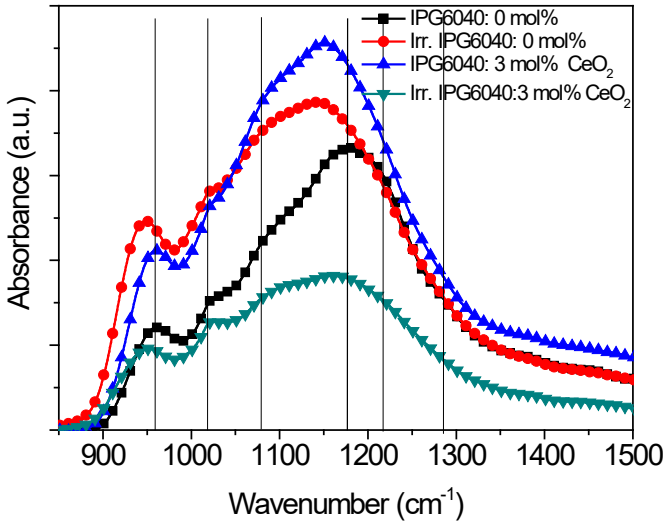

Figure 5: FTIR spectra for 0 mole% and 3 mole% CeO_2 doped IPG6040 samples before and after irradiation.

The shift of band towards lower wavenumber for cerium doped sample is attributed to existence of covalent bonds between cerium and non-bridging oxygen [11]. In addition, the shift of peaks towards lower wavenumber for irradiated 0 mole% and 3 mole% CeO_2 doped IPG samples, indicates decrease in bond angle for irradiated samples. The shift of peaks towards lower wavenumber for irradiated pure and CeO_2 doped IPG samples are attributed to ballistic damages caused by cascades of gold ions. This is in coherence with our previous findings [5].

Soft X-ray absorption spectroscopic measurements

SXAS is powerful technique to probe near surface regime. The iron L-edge X-ray absorption spectra for pure and CeO_2 doped iron phosphate glass samples before and after irradiation have been acquired in total electron yield mode, taking Fe_2O_3 as a reference sample. The reference sample is measured in parallel to IPG glass samples. Iron L-edge spectra for 0 mole% and 3 mole% CeO_2 doped IPG samples before and after irradiation with Fe_2O_3 reference sample are shown in figure 6. Local electronic structure, the oxidation state of X-ray absorbing atom, spin orbit coupling and crystal field splitting etc. decides the position and shape of the obtained peaks in XAS spectrum[12].

The origin of peaks in SXAS spectra (as seen in figure 6) are due to electronic transitions from Fe (2p) to hybridized O(2p)-Fe(3d) orbitals [13]. The peak with high intensity at lower energy is known as the L_3 edge, while the less intense peak at higher energy is called the L_2 edge. The spin orbit coupling is responsible for origin of L_3 and L_2 edges in SXAS spectra. The further splitting of L_3 and L_2 edges in SXAS spectra is due to crystal field splitting.

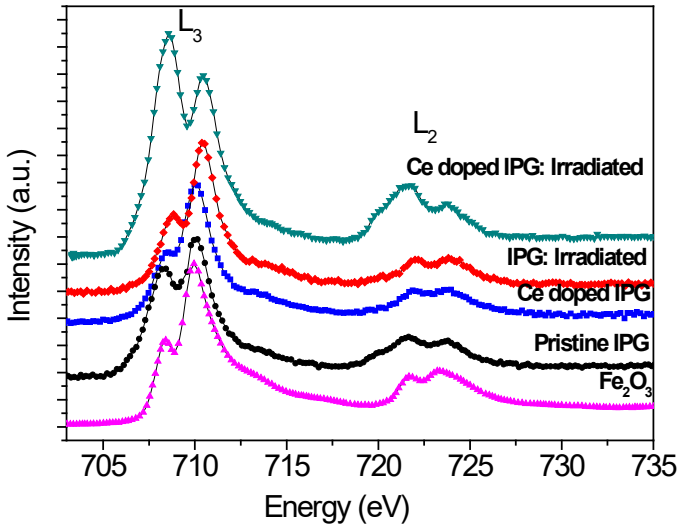

Fig. 6 Iron L-edge spectra for 0 mole% and 3 mole% CeO_2 doped IPG samples before and after irradiation.

Iron L_3 spectra of iron in mixed valence states always show two distinct maxima for Fe^{3+} and Fe^{2+} ions and the intensity ratio of these maxima changes with Fe^{3+} and Fe^{2+} iron content [14]. The first near edge peak for the obtained spectrum is characteristic of Fe^{2+} ions [15]. The intensity of peak corresponding to Fe^{2+} ions has increased for cerium loaded iron phosphate glass sample after irradiation. The observed significant iron reduction at ion energy of 750 keV for cerium loaded iron phosphate glass sample after irradiation may be attributed to

ballistic damage due to recoil atoms. Ray *et al.* have reported glass durability of 60 mol% P_2O_5-40 mol% Fe_2O_3 is independent of relative concentration of Fe^{3+} and Fe^{2+} iron content [16]. Later on, Fang *et al.* have reported that increase in Fe^{2+} content leads to formation of $Fe_3(P_2O_7)$ crystals in glass matrix [6]. Formation of $Fe_3(P_2O_7)$ crystals may lead to poor chemical durability of CeO_2 doped IPG samples. Nevertheless, heating effects due to energetic alpha particle during decay of actinides needs to be considered.

Conclusions

Irradiation experiments have been performed on pure and cerium doped iron phosphate glass samples. XRD patterns show amorphous nature of synthesised samples. Significant crystallisation is seen for 9 mole% CeO_2 doped iron phosphate glass sample. The new peaks appear in Raman spectra due to incorporation of cerium as a modifier in iron phosphate glass sample. In addition, infrared spectroscopic measurements indicate presence of covalent bonds between cerium and non-bridging oxygen. Electron microscopic investigation confirms formation of good quality bubble free glasses. In order to investigate irradiation induced damages lying close to sample surface, infrared and iron L-edge X-ray absorption spectroscopic measurements have been performed. Infrared spectroscopic measurement indicate shift of peaks towards lower wavenumber for irradiated pure and CeO_2 doped IPG samples. The observed shift is due to irradiation induced damages caused by cascades of gold ions. X-ray absorption spectroscopic spectra show insignificant iron reduction for pure IPG sample after irradiation. However significant iron reduction is observed in cerium doped IPG sample. Iron reduction may lead to formation of crystals, which can lead to poor chemical durability of CeO_2 doped IPG samples. It may pose threat to integrity of nuclear waste containing IPG samples. Future studies can be made to study synergetic effect of ballistic damage due to daughter nuclei and heating effects of alpha particles.

Acknowledgements

The research work was supported by EPSRC (Grant number: EP/I012214/1 and EP/K007882/1) and authors are thankful to The Royal Academy of Engineering and Nuclear Decommissioning Authority for financial support. Help from Dr. Dinesh Shukla from Raja Ramanna Centre for Advanced Technology, Indore, India is gratefully acknowledged for SXAS measurements on beamline 1, Indus 2 at RRCAT.

Reference(s):

1. Weber W. J. *et al.* (1997) Radiation effects in glasses used for immobilization of high-level waste and plutonium disposition. J. Mater. Res. 12: 1946-1978.
2. Mann C. *et al.* (2019) Influence of young cement water on the corrosion of the International Simple Glas. npj Materials Degradation. 5:1-9.
3. Mir A. H. *et al.* (2016) Mono and sequential ion irradiation induced damage formation and damage recovery in oxide glasses: Stopping power dependence of the mechanical properties. J. Nucl. Mater. 469: 244-250.
4. Yu X. *et al.* (1997) Properties and structure of sodium-iron phosphate glasses. J. Non-Cryst. Solids. 215:21-31.
5. Dube C. L. *et al.* (2016) Simulation of alpha decay of actinides in iron phosphate glasses by ion irradiation. Nucl. Instru. Meth. Phy. Res. B 371: 424–428.
6. Fang X. *et al.*(2001) Iron redox equilibrium, structure and properties of iron phosphate glasses. J. Non-Cryst. Solids 283:162-172.
7. Dube C. L. *et al.* (2015) Positron annihilation lifetime measurement and X-ray analysis on
120 MeV Au+7 irradiated polycrystalline tungsten. J Nucl. Mater. 467 (1): 406-412.
8. Wang F. *et al.* (2015) Glass formation and FTIR spectra of CeO2-doped 36Fe2O3–10B2O3–54P2O5 glasses. J. Non-Cryst. Solids 409:76–82.
9. Ziegler J. F. *et al.* the Stopping and Range of Ions in Solids, Pergamon Press, New York, 1985.
10. Dube C. L. (2017) Fourier Transform Infrared Spectroscopy: Fast and Versatile Technique for Chemical Characterization J. Fibre to Finish, 56(1).
11. Lai Y. M. *et al.* (2011) Raman and FTIR spectra of iron phosphate glasses containing cerium J. Mol. Str. 992:84-88.
12. Lobacheva O. *et al.* (2014) The local structure and ferromagnetism in Fe-implanted SrTiO3 single crystals. J. Appl. Phys. 116: 013901-1-013901-5.
13. Shen S. *et al.* (2014) Surface Engineered Doping of Hematite Nanorod Arrays for Improved Photoelectrochemical Water Splitting. Scientific reports 4: 6627-1-6627-9.
14. Aken P. A. V. *et al.* (2002) Quantification of ferrous/ferric ratios in minerals: new evaluation schemes of Fe *L23* electron enrgy-loss near-edge spectra. 29:188-200.
15. Booth C. H. *et al.* (1999) Phosphorus coordination around iron in crystalline ferric ferrous pyrophosphate and iron-phosphate glasses with UO2 or Na2O. J. Mater. Res., 14:2628-2639.

16. Ray C. S. *et al.* (1999) Effect of melting temperature and time on iron valence and crystallization of iron phosphate glasses. J. Non-Cryst. Solids 249: 1.